Journal of The
Electrochemical Society

The Electrochemical Society
Advancing solid state & electrochemical science & technology

Effects of Electrolyte Composition on Lithium Plating in Lithium-Ion Cells

To cite this article: M. C. Smart and B. V. Ratnakumar 2011 *J. Electrochem. Soc.* **158** A379

View the article online for updates and enhancements.

You may also like

- Modeling of Lithium Intercalation in Twisted Bilayer Graphene
Victor Venturi and Venkatasubramanian Viswanathan

- Material and Electrochemical Characterization of Tetrapropylammonium Manganese Oxide Thin Films as Novel Electrode Materials for Electrochemical Capacitors
Suk-Fun Chin, Suh-Cem Pang and Marc A. Anderson

- A Mechanistic Study on Lead-Induced Passivity-Degradation of Nickel-Based Alloy
B. T. Lu, J. L. Luo and Y. C. Lu

Watch Your Electrodes Breathe!

EL-CELL®
electrochemical test equipment

Measure the Electrode Expansion in the Nanometer Range with the ECD-4-nano.

- Battery Test Cell for Dilatometric Analysis (Expansion of Electrodes)
- Capacitive Displacement Sensor (Range 250 µm, Resolution ≤ 5 nm)
- Detect Thickness Changes of the Individual Half Cell or the Full Cell
- Additional Gas Pressure (0 to 3 bar) and Temperature Sensor (-20 to 80° C)

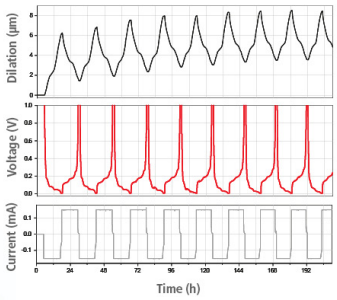

See Sample Test Results:
Scan me!

Download the Data Sheet (PDF):
Scan me!

Or contact us directly:
+49 40 79012-734
sales@el-cell.com
www.el-cell.com

This content was downloaded from IP address 54.68.167.180 on 05/12/2024 at 16:36

Journal of The Electrochemical Society, **158** (4) A379-A389 (2011)
0013-4651/2011/158(4)/A379/11/$28.00 © The Electrochemical Society

Effects of Electrolyte Composition on Lithium Plating in Lithium-Ion Cells

M. C. Smart* **and B. V. Ratnakumar*,z**

Jet Propulsion Laboratory, California Institute of Technology Pasadena, California 91109, USA

Metallic lithium is typically absent in a lithium-ion (Li-ion) cell under normal conditions of operation. Under strenuous charge conditions of high charge rates and/or low temperatures, however, lithium metal will deposit on the carbon anode in preference to lithium intercalation, especially after considerable cycling and storage, which contribute to the degradation of anode capacity. Such plated lithium will react more readily in the Li-ion battery electrolytes and pose problems related to performance, reliability, and safety of the cell. Factors that affect the anode performance, specifically its polarization and lithium intercalation kinetics, play a crucial role in determining the propensity for lithium deposition. Such factors include the nature of solid electrolyte interphase (SEI), which is in turn governed by the electrolyte constituents, anode/cathode capacity ratios, and the operating conditions. In this paper, the Li intercalation kinetics and their impact on Li plating were studied with two sets of electrolytes containing different proportions of EC and with SEI-stabilizing additives. Electrolytes with low EC-formulations and those without SEI-stabilizing additives are relatively immune to lithium plating.
© 2011 The Electrochemical Society. [DOI: 10.1149/1.3544439] All rights reserved.

Manuscript submitted September 28, 2010; revised manuscript received December 21, 2010. Published February 22, 2011.

Lithium-ion (Li-ion) cells have been so named[1] for the reason that the reactions occurring at both anode and cathode, during charge or discharge, involve only intercalation[2] of lithium ions into the galleries of lithiated metal oxide cathodes and carbonaceous anodes. Lithium ions thus shuttle from cathode to anode on charge and vice versa on discharge. There is no likelihood of lithium being present in metallic form and contributing to the faradic process via its deposition and dissolution processes at the anode, under normal operating conditions. Several probing techniques have been adopted in the literature to understand the nature of lithium in the host electrodes, which reveal that the lithium is largely ionic in nature, even though its electrochemical potential is proximate to the lithium reversible potential, especially in graphite. For example, ^{7}Li NMR measurements show the knight shift for intercalated Li is around 270 ppm as compared to about 1350 for metallic Li.[3] The electron energy loss spectroscopy (EELS) measurements performed by Fultz and co-workers, however, show more proximate energy values for the intercalated lithium and metallic lithium.[4] Although the electrochemical processes at anode and cathode are largely the same as designed and desired under normal conditions, there is a likelihood of additional parasitic reactions occurring at both the electrodes, especially upon aging. For example, there is a possibility for an oxidation of electrolyte species at the cathode, in the latter durations of charge, particularly at high charge voltages. More importantly, under similar conditions, metallic lithium could be deposited on the carbonaceous anode, in place of Li intercalation, especially at low temepratures.[5]

This tendency toward Li plating is a strong function of cell design parameters as well as operating conditions. Anode materials that have high reversible potentials (more positive to lithium), for example, coke, will be more immune to such lithium plating, while graphite will be more susceptible with its reversible potential close to that of the lithium deposition potential (i.e., within 100 mV). Furthermore, the ratio of the anode capacity to the cathode capacity is a critical parameter in distributing the overall cell polarization into individual overpotentials impressed at the electrodes. Li-ion cells are generally designed with excess anode capacity to avoid depletion of intercalation sites in the anode and thus to minimize such an overpotential at the anode. However, the cathode proportion is often increased to maximize the specific energy and energy density values of the cells, which would increase their susceptibility toward lithium plating. Further, the higher capacity fade in graphite compared to metal oxide cathodes may decrease anode reserve upon cycling and/or storage, thus paving way for lithium plating.

Lithium deposition has also been studied through first-principles based mathematical models. Aurora et al.[6] described lithium deposition in Li_xC_6:Li_yMnO_2 system through modeling, using macrohomogeneous approach, which, however, does not capture edge effects adequately. The edge effects have been experimentally shown by Scott et al.[7] to be significant, i.e., ~1 V of potential difference within the electrolyte from the center of the cell to the edge of the coil. It was also shown experimentally that lithium deposition might occur at the edges of electrodes even under conditions not favorable for lithium plating. Newman and co-workers[8] have examined the current distribution during charge to explain how such lithium plating can be avoided by extending the negative electrode geometrically beyond the positive electrode.

In contrast to the designed ratio of electrode capacities and electrode geometries, the utilization of the anode could be lower from kinetic considerations, i.e., due to slower Li intercalation kinetics at the anode, especially at low temperatures,[9,10] which are largely governed by the nature of electrolyte. Based on several studies performed at the Jet Propulsion Laboratory (JPL) (Ref. 11) and elsewhere,[12] it is evident that the electrolyte plays a strong role in defining the interfacial conditions at the anode and in determining the SEI properties on its surface. In addition to the nature of the electrolyte and anode, the operating conditions also play a crucial role. For instance, experimental conditions that would relatively impede lithium intercalation kinetics at the anode compared to the cathode, e.g., low temperatures, would facilitate lithium plating at the anode. As well, high charge rates and high charge voltages, particularly at subambient temperatures, tend to polarize the anode to potentials amenable to Li plating.

There is no consistent understanding on the effects of plated lithium on subsequent durability of cells. It is possible that the lithium thus plated may intercalate "chemically" into graphite, given sufficient time, as contended by some researchers.[10,13] However, it is our experience that the presence of metallic Li on the anode generally leads to further degradation in the anode/electrolyte interface. Li metal is known to be very reactive toward electrolytes, and based on many unsuccessful attempts in the past to stabilize Li metal anodes in organic electrolytes, it is reasonable to infer that such lithium plating will pose serious problems, both in terms of performance and[14,15] reliability and safety of Li-ion cells. The recent studies at Exponent, Inc., based on a destructive physical analysis study of commercial Li-ion cells,[16] indicate that dendrite shorting was observed to occur in cells as a result of lithium plating, consistent with other reports in the literature. It was reported that the plating could occur in commercial cells due to a variety of manufacturing problems, as well as usage and aging scenarios (Fig. 1). Further, the accelerated rate calorimetry (ARC) tests on cells with plated lithium

* Electrochemical Society Active Member.
z E-mail: ratnakumar.v.bugga@jpl.nasa.gov

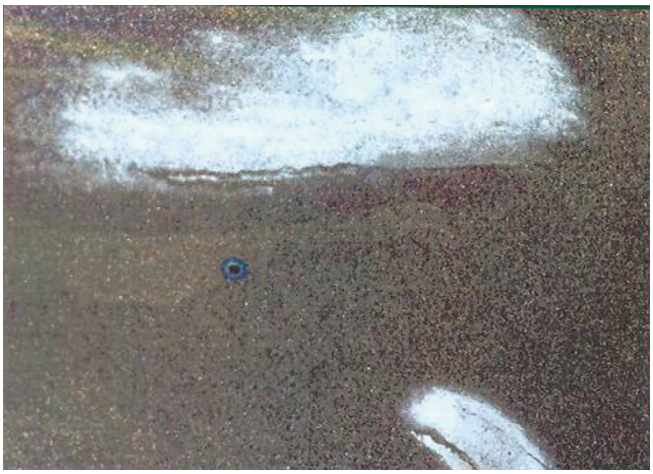

Figure 1. Lithium plating on graphite evident form a micrograph of the anode retrieved a commercial cell.[16]

exhibited no appreciable change in reactivity below lithium melting temperature, but a sharp isotherm near lithium melting temperatures, much like with lithium primary cells, thus underlying the safety issues. Finally, it was postulated that lithium plating can enhance the likelihood of cell thermal runway, due to the formation of a mat of "inaccessible or dead lithium" proximate to a lithium dendrite.

Our previous studies indicate that the lithium intercalation kinetics are mainly dictated by the anode surface films (SEI), which in turn could be controlled by a judicious selection of electrolyte solution, i.e., either the solvent type or salt type.[17] In this paper, we illustrate the strong effect of electrolytes in determining the Li intercalating kinetics at the anode and thus, in turn, affecting the onset of Li plating. Such effects are further demonstrated in prototype cells, containing different electrolytes. Likewise, the effects of reduced anode to cathode capacities in facilitating conditions favorable for Li plating are demonstrated in prototype cells. Finally, the combined effects of the charge rate as well as charge temperature on the propensity for Li plating have been examined in various prototype cells, with different electrolytes and designs, which were described in detail in our recent publication.[14]

Experimental

The effects of different electrolytes on lithium plating were determined in three-electrode, O-ring-sealed, glass cells containing spiral rolls of mesocarbon microbead (MCMB) 1028 graphite anodes, $LiNi_{0.8}Co_{0.2}O_2$ cathodes, and lithium reference electrodes separated by two layers of porous polyethylene. Both the anodes and cathodes for the laboratory cells were supplied by Yardney Technical Products (or Lithion), Pawcatuck, CT. The electrolytes contained carbonate-based solvents, including ethylene carbonate (EC), dimethyl carbonate (DMC), diethyl carbonate (DEC), and ethyl methyl carbonate (EMC), with $LiPF_6$ salt in the desired concentration, and were purchased from Mitsubishi or Ferro Corporation with less than 50 ppm of water. The capacities of these cells are typically around 300–400 mAh at 25°C. The dc electrochemical measurements were performed using an EG&G Potentiostat/Galvanostat interfaced with an IBM PC, using Softcorr 352. Charge–discharge measurements and cycling tests were carried out on these test cells with an Arbin battery cycler. A Tenney environmental chamber was used to maintain the desired temperature within ±1°C for the cells (convectively cooled).

Results

As mentioned above, the reversible potential for lithium intercalation/deintercalation is a function of the lithium content, as is evident from various voltage plateaus observed during lithiation, termed also as staging.[18,19] The potential of a fully lithiated graphite ($Li_{0.166}C$) anode is typically around 85–100 mV vs Li. It may noted that the corresponding potential for coke is ~500 mV from Li, sufficiently far away from the Li reversible potential to pose any problem of Li plating. Because oxidation (stripping) of lithium is a more facile reaction than Li deintercalation, there are two distinct voltage plateaus corresponding to these processes in the subsequent discharge. In other words, the presence of metallic Li covering a graphite anode leads to a higher voltage plateau (upon "stripping") preceding the expected discharge curve, without such Li plating, as illustrated in Fig. 2.[5] It may be seen from the figure that the plateau is wider with increased Li plating, as is the case after successive charges at low temperatures. Using the high voltage plateau as the signature for Li plating, we have examined various experimental conditions, i.e., with different electrolytes to assess their vulnerability.

Effect of relative kinetics for Li intercalation versus plating.— For a semiquantitative understanding of the effect of relative kinetics for Li intercalation and Li plating, a brief analysis has been carried out here, based on simplified electrochemical rate equations. During constant current charging, the applied current at the anode, i_a, as well as the current flowing through the cathode, i_c, are the same as the applied cell current, i_{cell}.

$$i_{cell} = i_a = i_c \quad [1]$$

The current at the anode, i_a is divided between the currents from lithium intercalation into the carbonaceous anode, $i_{a,I}$, and from lithium plating over the anode surface, $i_{a,p}$

$$i_a = i_{a,i} + i_{a,p} \quad [2]$$

It is assumed here that there has not been any onset of lithium plating on the anode yet, such that the anode equilibrium potential is the same as reversible potential of the Li intercalation. If there is already metallic Li present on the anode surface, its potential will then be a mixed potential between the potentials of intercalated Li (into carbon) and metallic Li. The relation between the current and the anode potential may be expressed by a simplified electrochemical rate equation, also termed as the Butler–Volmer equation, without the mass transfer effects as[20]

$$\frac{i}{i_o} = \left\{\exp\left(\frac{-\alpha nF}{RT}(E - E_{equi})\right)\right\} - \left\{\exp\left(\frac{(1-\alpha)nF}{RT}(E - E_{equi})\right)\right\} \quad [3]$$

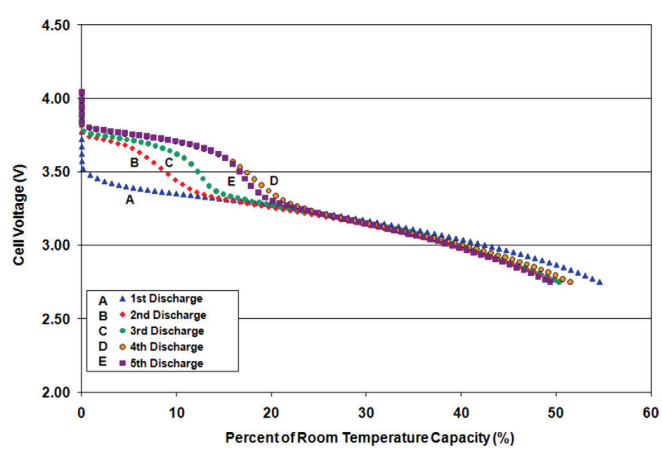

Figure 2. Discharge curves of a Li-ion cell at C/20 at –40°C, after charging at 25°C (A) at C/20 to 4.1 V followed by taper to C/50, and after charging at –40°C in subsequent (B) second, (C) third, (D) fourth, and (E) fifth discharges.

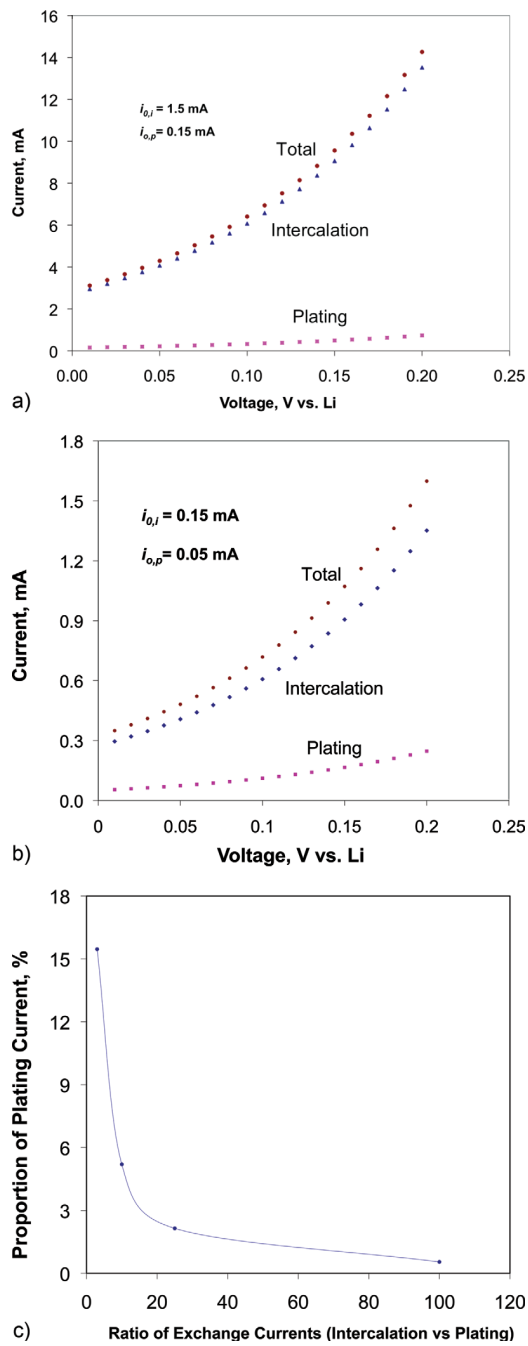

Figure 3. Estimated contributions from: (1) total anodic currents, (2) Li intercalation into carbon and (3) Li plating on the anode in the, when the exchange currents for the intercalation and plating are (a) 1.5 and 0. 15 mA and (b) 0.15 and 0.05 mA, respectively. In case (a), Li intercalation process is ten times faster, whereas in case (b), it is only three times faster. (c) The proportion (%) of the current contributed by the plating process at different ratios of exchange currents for intercalation to plating.

where i is the current density, i_o is the exchange current density of the reaction, α is the cathodic energy transfer coefficient, n is the number of electrons involved in the charge transfer process, E is the applied electrode potential (versus Li) and E_{equi} is the equilibrium electrode potential (versus Li). For the sake of approximation, the effects of mass transfer are ignored here, which will probably be more significant for Li intercalation compared to lithium plating, due to a slow diffusion of lithium ions in the galleries of carbon.

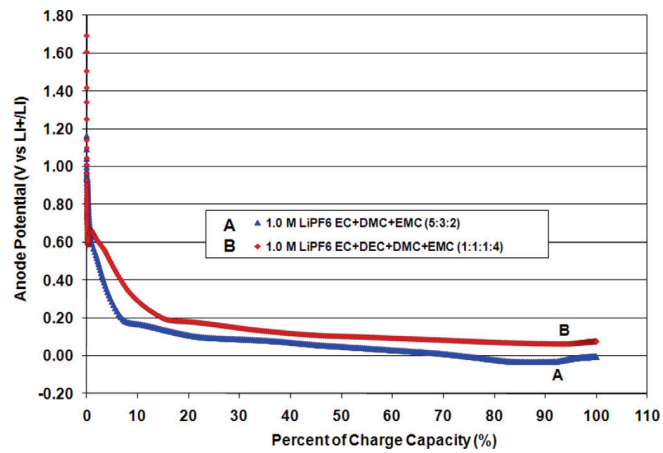

Figure 4. Anode potentials during formation of MCMB-NCO Li-ion test cells with electrolytes containing 1 M $LiPF_6$ in (A) high EC, i.e., 5:3:2 EC:DMC:EMC mixture and (B) low EC, i.e., 1:1:1:4 EC:DMC:DEC:EMC mixture, during first charge at 25 mA to 4.1 V at ambient temperature.

The individual currents for Li-ion intercalation may thus be expressed as

$$\frac{i_i}{i_{o,i}} = \left\{\exp\left(\frac{-\alpha_i n_i F}{RT}(E - E_{equi,i})\right)\right\} - \left\{\exp\left(\frac{(1-\alpha_i) n_i F}{RT}(E - E_{equi,i})\right)\right\} \quad [4]$$

Again, it is reasonable to assume that during charging process, the cathodic overpotentials are significant at the anode for Li intercalation, such that the anodic process of deintercalation may be ignored. In other words, the reaction may be assumed to be in the Tafel regime, which reduces the above equation to

$$\frac{i_i}{i_{o,i}} = \left\{\exp\left(\frac{-\alpha_i n_i F}{RT}(E - E_{equi,i})\right)\right\} \quad [5]$$

The corresponding equation for Li plating may be expressed as

$$\frac{i_p}{i_{o,p}} = \left\{\exp\left(\frac{-\alpha_p n_p F}{RT}(E)\right)\right\} \quad [6]$$

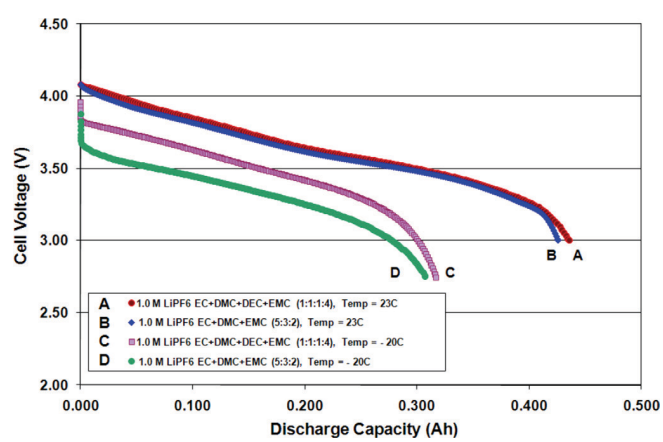

Figure 5. Discharge performance of MCMB-$LiNi_xCo_{1-x}O_2$ Li-ion test cells with electrolytes containing 1 M $LiPF_6$ in (A) high EC, i.e., 5:3:2 EC:DMC:EMC mixture and (B) low EC, i.e., 1:1:1:4 EC:DMC:DEC:EMC mixture at 25 mA. Curves (C) and (D) represent the corresponding discharges at –20°C. The cells were charged at 25 mA to 4.1 V, followed by taper charge to C/100 at 25°C.

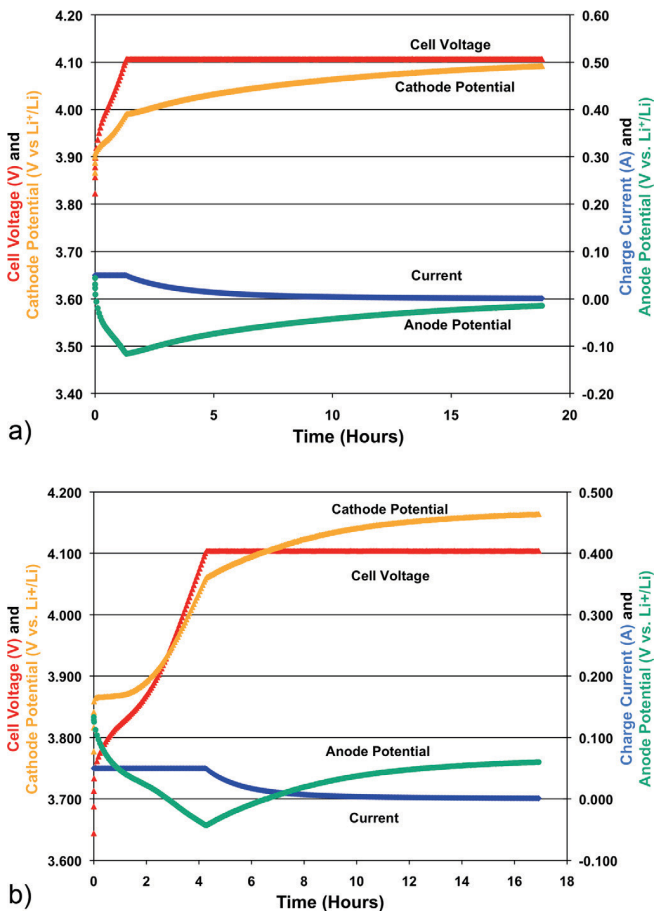

Figure 6. (1) Cell potentials, (2) cell currents, (3) individual cathode, and (4) anode potentials in MCMB-NCO Li-ion test cells with electrolytes containing 1 M $LiPF_6$ in (a) high EC, i.e., 5:3:2 EC:DMC:EMC and (b) low EC, i.e., 1:1:1:4 EC:DMC:DEC:EMC mixtures, during charging at –20°C at 50 mA to 4.1 V followed by taper.

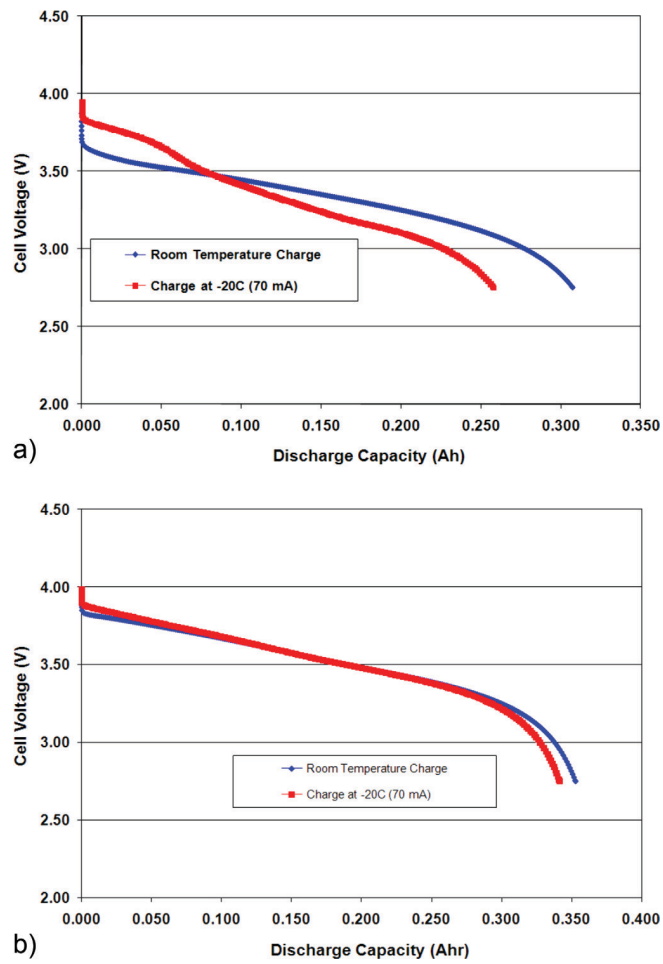

Figure 7. Discharge curves of MCMB-NCO Li-ion test cells with electrolytes containing 1 M $LiPF_6$ in (a) high EC, i.e., 5:3:2 EC:DMC:EMC mixture and (b) low EC, i.e., 1:1:1:4 EC:DMC:DEC:EMC mixture, at 25 mA and −20°C, following charge at 70 mA at room temperature and –20°C.

Note that the reversible potential term is missing here, because all the electrode potentials are expressed against Li electrode. Adding the currents from intercalation and plating processes, the total anodic current or the cell current may be expressed as

$$i_{\text{cell}} = i_{\text{o,i}}\left\{\exp\left(\frac{-\alpha_{\text{i}} n_{\text{i}} F}{RT}(E - E_{\text{equi,i}})\right)\right\} + i_{\text{o,p}}\left\{\exp\left(\frac{-\alpha_{\text{p}} n_{\text{p}} F}{RT}(E)\right)\right\} \quad [7]$$

The above expression describes the current–voltage characteristics of anode during charging, especially toward the end of charging. The applied current is thus divided between the intercalation current and plating current. If all the current can be supported by the intercalation current, without driving the electrode potential negative to the lithium electrode potential, there would not be any Li plating. If the anode potential drops below the lithium electrode potential, there is a dynamic balance and sharing between the intercalation current and plating current that would in turn define the anode potential and thus the cell voltage.

Using Eq. 7, the currents corresponding to the intercalation and Li plating may be calculated at various electrode potentials, especially at potentials lower than Li^+/Li. Figures 3a and 3b illustrate the estimated currents from Li intercalation and Li plating processes in two different hypothetical scenarios, i.e., with different values and ratios for the exchange currents corresponding to the intercalation and plating processes. A Tafel slope of 0.125 V was assumed here both for the intercalation and plating processes. Figure 3a corresponds to a case where the exchange current for the Li intercalation is about ten times higher than that of the plating reaction, i.e., 0.0015 and 0.00015 A for Li intercalation and Li plating reactions, respectively. This is likely to be case under ambient conditions, wherein the anode current is mostly contributed by Li intercalation, even at potentials negative to Li. Figure 3b describes the scenario where the exchange currents of both the processes are considerably reduced, more prominently for the intercalation process as compared to plating. Specifically, the values chosen for $i_{\text{o,i}}$ and $i_{\text{o,p}}$ are 0.00015 and 0.00005 A, respectively, i.e., the intercalation process is slowed down ten times compared to Fig. 3a, while the plating process is only reduced by three times. Under these conditions, a higher proportion of current would be generated from the plating process. This is typically what happens at low temperatures, with the intercalation process more hindered compared to Li plating, due to poor interfacial properties of the graphitic anodes. Figure 3c illustrates the variation of the contribution from the plating process with the relative rates (exchange currents) of intercalation and plating processes. As the ratio of exchange currents for intercalation and plating decreases, the proportion of the plating current in the overall anodic current increases.

Effect of electrolyte on Li plating.—It is thus clear from the above discussion that a reduction in the lithium intercalation kinetics, especially at low temperatures, is responsible for lithium plating on the anode during charging. We have shown in several of

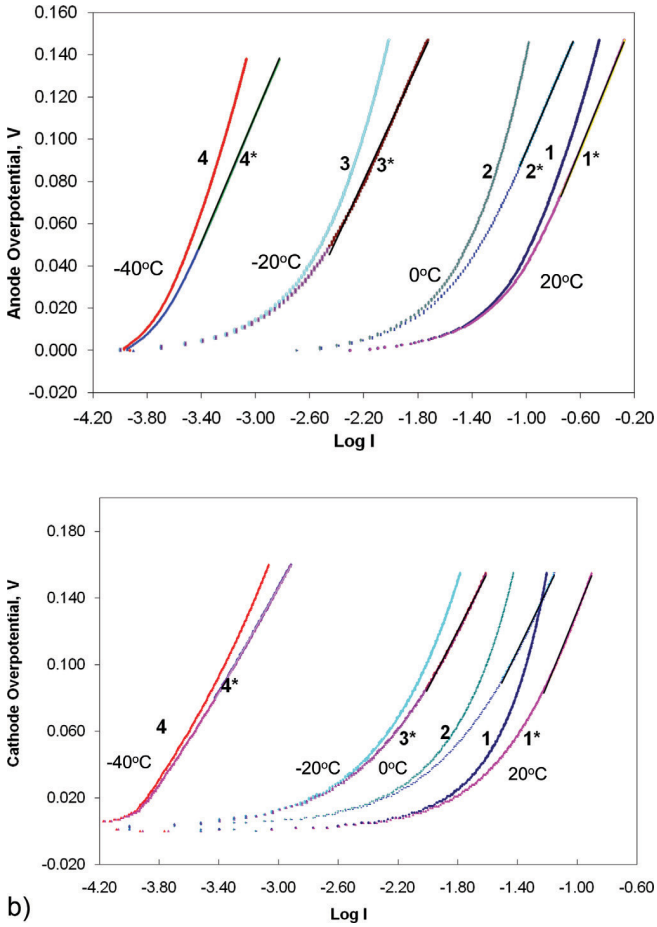

Figure 8. Tafel curves of (a) anode and (b) cathode in high EC-electrolyte, i.e., 1 M $LiPF_6$ in 5:3:2 EC:DMC:EMC mixture at (1) 25°C, (2) 0°C, (3) –20°C, and –40°C. Also included here are the corresponding corrected (corrected for mass transfer effects) Tafel plots, designated as 1*, 2*, 3*, and 4*, respectively.

our earlier publications[17,20] that the electrolyte is a strong determining factor for the lithium intercalation kinetics, especially at the anode. A good low temperature electrolyte will not only facilitate rapid ionic mobility at low temperatures, due to its high conductivity and low viscosity, but also provide favorable interfacial SEI characteristics on the anode, such that Li intercalation process is facilitated. Such an electrolyte is thus expected to minimize or eliminate the problem of lithium plating during low temperature charging. Here are a couple of examples that will illustrate the strong impact of the electrolyte lithium plating.

Electrolyte formulations with low EC and high EC contents.—Two electrolyte formulations, i.e., with 1.0 M $LiPF_6$ dissolved in solvents with high and low EC contents, specifically (i) a ternary mixture of EC, DMC, and EMC in a volume ratio of 5:3:2 (termed as high-EC formulation) and (ii) a quaternary mixture of EC, DMC, DEC, and EMC in a volume proportion of 1:1:1:4 (termed as low-EC formulation) were chosen as examples here. The first electrolyte formulation provides a good cyclic stability at ambient and warm temperatures and was used by the battery manufacturers. The second formulation represents one of JPL's electrolytes for improving the low temperature performance.[20] Good low temperature performance was observed with this electrolyte down to –60°C in laboratory test cells. The high-EC formulation, on the other hand, is deemed to be good for long cycle life but exhibits a relatively poor low temperature performance. Three-electrode cells were fabricated with the above electrolyte solutions, with MCMB anodes and lithiated nickel cobalt oxides cathodes supplied by Yardney Technical Products and with Li reference electrodes, to derive basic electrochemical data on individual electrode kinetics at different temperatures.

Figure 4 shows the first charge during the formation process of these cells containing electrolytes based on high-EC and low-EC solvent mixtures. The first lithiation process of the anode indicates the ability of the electrolyte to film the anode and form an SEI in the desirable configuration. A thin and coherent SEI formed by consuming less lithium is expected to be more favorable for the subsequent lithium intercalation. A bulky SEI formed by consuming considerable lithium is unlikely to be protective enough, such that it continues to grow during subsequent cycling. As may be seen from the figure, the SEI formation is facially rapid in both the solutions, as evident by the rapid voltage decline to values typical of lithium intercalation. However, because EC is known to be the predominant component responsible for the SEI formation on graphite, the solution with high-EC proportion facilitates more rapid SEI formation and also relatively lower intercalation potentials.

As may be expected, the cell containing the electrolyte with a low-EC proportion in the solvent mixture performs better than its counter part with a high-EC proportion solvent mixture at low temperatures (Fig. 5). Even though the reversible capacities at room temperature are nearly identical, their capacities at low temperatures, e.g., –20°C, and a discharge rate of ~C/16 are noticeably different even at low rate, with the low-EC solutions providing higher capacity, also with higher discharge voltages, compared to the high-EC solution. This improvement in the low temperature performance, which is more dramatic at higher rates and lower temperatures, also reported in our previous publications, is not only due to the improved mobility for lithium ions in the low-EC solutions but also more notably due to the improved interfacial properties in such solutions.

There are more interesting differences between these two cells during charging, especially at low temperatures. Figure 6a shows the individual electrode potentials, cell voltage, and cell current during charging at 50 mA (about C/8) at –20°C for the cell containing

Table I. Kinetic parameters for Li intercalation in graphite and deintercalation from NCO cathode in different electrolytes.

		Tafel parameters							
		Tafel slopa				Exchange current, mA			
Electrolyte	Electrode	25°C	0°C	−20°C	−40°C	25°C	0°C	−20°C	−40°C
1,0 M LiPF6 EC:DEC:DMC:EMC (1:1:1:3 vol%)	Cathode	0.18	0.17	0.16	0.16	26.00	8.20	0.40	020
	Anode	0.13	0.16	0.14	0.13	124.00	50.60	5.96	0.17
1.0 M LIPF6 EC+DMC+EMC (5:3:2 vol%)	Cathode	0.22	0.17	0.18	0.16	24.80	16.20	3.23	0.18
	Anode	0.16	0.14	0.15	0.15	61.80	23.70	1.66	0.18
1.0 M LiPF6 EC+DMC+DEC +EMC (1:1:1:4 vol %)	Cathode	0.18	0.17	0.15		26.60	11.10	2.46	
	Anode	0.14	0.18	0.16		427.00	135.90	16.60	
1.0 M LiPF6 EC+DEC+DMC+EMC (1:1:1:4 vol %) +-VC	Cathode	0.13	0.14	0.13		27.30	11.84	2.35	
	Anode	0.11	0.15	0.15		152.00	41.50	4.35	

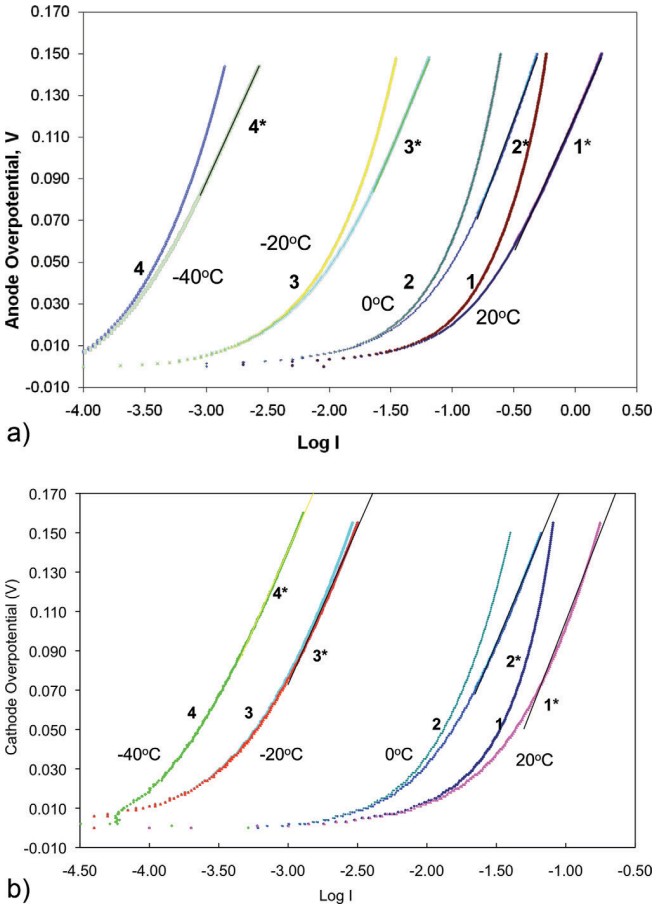

Figure 9. Tafel curves of (a) anode and (b) cathode in low-EC electrolyte, i.e., 1 M $LiPF_6$ in 1:1:1:4 EC:DMC:DEC:EMC mixture, at (1) 25°C, (2) 0°C, (3) –20°C, and –40°C. Also included here are the corresponding corrected (corrected for mass transfer effects) Tafel plots, designated as 1*, 2*, 3*, and 4*, respectively.

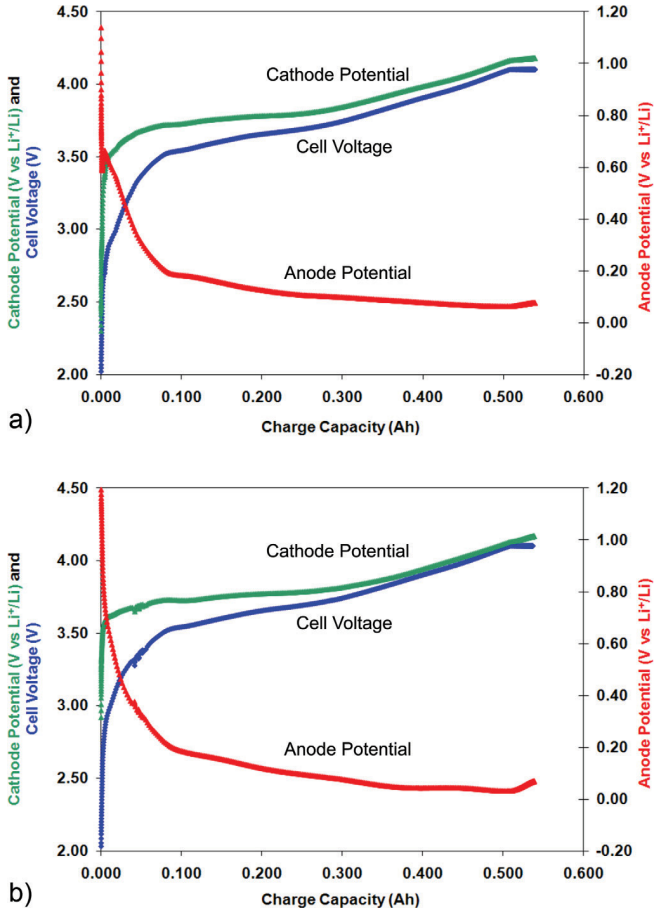

Figure 10. (1) Cell potentials, (2) cathode, and (3) anode potentials in MCMB-NCO Li-ion test cells with electrolytes containing 1 M $LiPF_6$ in (a) EC:DMC:DEC:EMC (1:1:1:4) without VC and (b) with VC additive charging at 23°C at 25 mA to 4.1 V followed by taper.

the high-EC proportion. The cathode potential exhibits the normal trend, i.e., to increase steeply during constant current charging, followed by a relatively slow increase in the constant voltage or tapered charge mode. The anode potential, on the other hand, has considerable undershoot, even below the lithium potential. The voltage goes as low as − 120 mV vs Li and never relaxes to the positive potentials even though current continues to taper. For the entire duration of the charge, the anode potential is negative to the Li^+/Li potential, which suggests a possibility for noticeable Li plating on the anode. The cell containing the electrolyte with low-EC solvent mixture (Fig. 6b) also exhibits an undershoot in the anode potential, but only for a short period at the end of the constant current charging. The anode potential becomes the most negative (approximately –70mV vs Li^+/Li), when the charge voltage and current are highest. Once the cell gets into tapered charge mode, the anode potential quickly recovers and remains in the positive territory (∼0.05 V vs Li^+/Li). Interestingly, the cathode is more polarized here, by about 50 mV, suggesting that the cell polarization is distributed more uniformly here between the anode and cathode, unlike the cell with high-EC solution. Based on the sustained heavy polarization of the anode in the high-EC solution, there might be some noticeable lithium plating during this charge process.

Figures 7a and 7b display the discharge characteristics at –20°C, following the charging similar to that illustrated in Figs. 6a and 6b. As expected from its charge behavior, the cell with high-EC content electrolyte has pronounced lithium plating, evident from a high voltage plateau. It may be noted that the voltage corresponding to the lithium stripping is considerably higher than 100 mV, expected from their open-circuit potentials. This may be attributed to a likely lower overpotential and facile kinetics for lithium oxidation (stripping) compared to lithium deintercalation at this temperature. When the charging was done at room temperature, however, there was no plating of lithium as evident from the absence of a high voltage plateau.

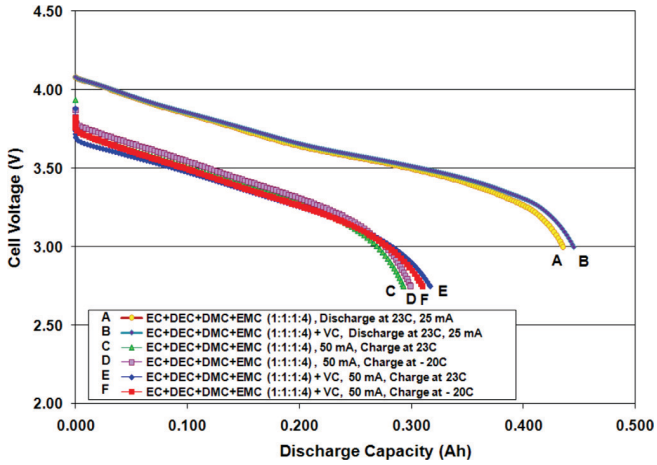

Figure 11. Performance of MCMB-NCO Li-ion test cells with electrolytes containing 1 M $LiPF_6$ in (A) EC:DMC:DEC:EMC (1:1:1:4) without VC and (B) with VC additive at –20°C.

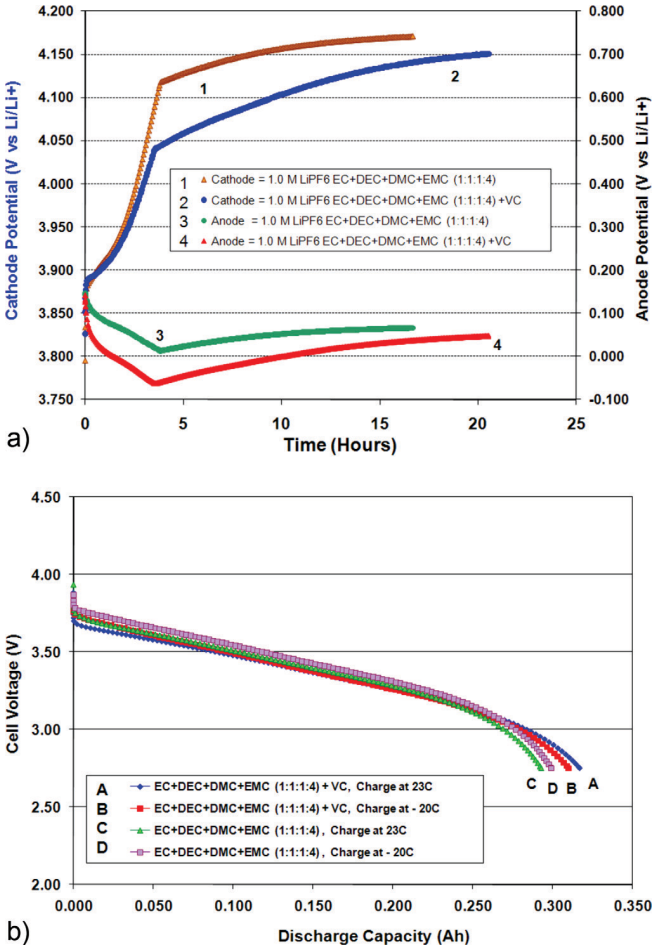

Figure 12. (a) Cathode and anode potentials in MCMB-NCO Li-ion test cells with electrolytes containing 1 M $LiPF_6$ in EC:DMC:DEC:EMC (1:1:1:4) without VC and with VC additive during charging at –20°C at 50 mA to 4.1 V followed by taper. (b) Discharge curves of MCMB-NCO Li-ion test cells with electrolytes containing 1 M $LiPF_6$ in EC:DMC:DEC:EMC (1:1:1:4) with and without VC additive at 50 mA, after charging at 23 and –20°C.

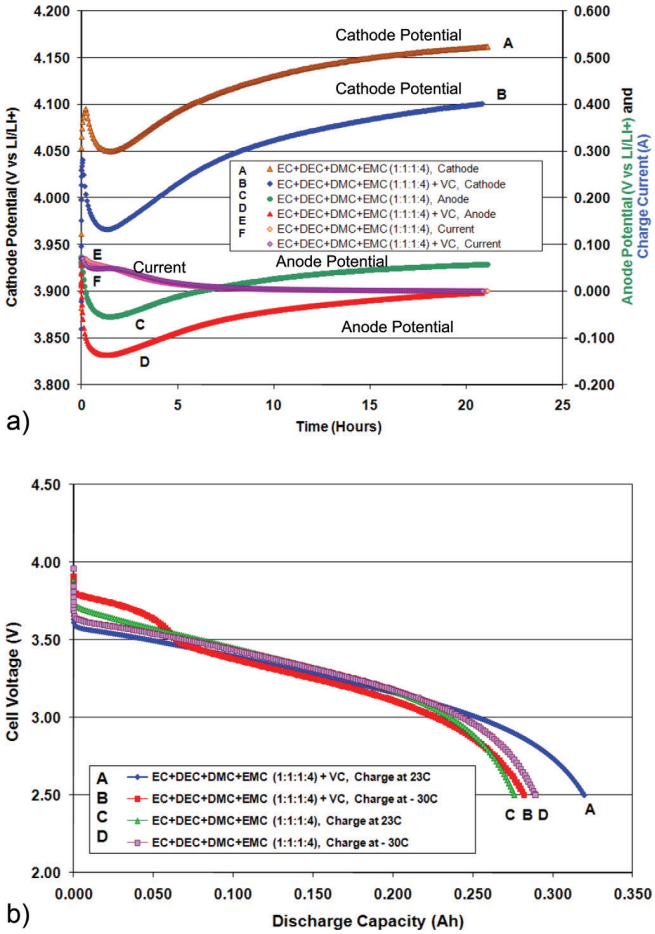

Figure 13. (a) Cathode and anode potentials in MCMB-NCO Li-ion test cells with electrolytes containing 1 M $LiPF_6$ in EC:DMC:DEC:EMC (1:1:1:4) without VC and (B) with VC additive during charging at –30°C at 50 mA to 4.1 V followed by taper. (b) Discharge curves of MCMB-NCO Li-ion test cells with electrolytes containing 1 M $LiPF_6$ in EC:DMC:DEC:EMC (1:1:1:4) with and without VC additive at 25 mA, after charging at 23 and –30°C.

In contrast, the cell with low-EC content electrolyte does not exhibit any lithium plating at –20°C (Fig. 7b), again evident form the absence of the high voltage plateau. Although the anode potential became negative in the previous charge, no lithium plating was observed with this cell in the subsequent discharge profiles. This might be due to the fact that the potentials were not sufficiently negative and/or any lithium plated on the electrode surface could intercalate into the carbon during the taper mode.

Electrochemical kinetics.— In order to get more quantitative understanding of the kinetics for the lithium intercalation and plating processes in EC-rich and low-EC electrolyte solutions, we performed dc polarization measurements, specifically Tafel measurements, on the individual electrodes, as described below.

The Tafel data were generated on individual electrodes under pseudo-steady state conditions, i.e., at very slow scan rates of potentiodynamic polarization. The scan rates adopted are typically 0.5 mV/s, with the electrodes polarized from their open-circuit potentials to an overpotential of ~150–200 mV, in the positive direction for the anode and negative direction for the cathode. The measurements were conducted on the electrodes while they were in a full state of charge, i.e., with the cathode in a delithiated state and the anode in lithiated condition. Figures 8a and 8b illustrate the Tafel polarizations of anode and cathode in the EC-rich formulation, respectively. In all of these Tafel plots, there are distinct charge-transfer controlled regimes, where the overpotential increases linearly with log (I). However, in many cases, there is a considerable interference from mass transfer processes such that the current tends to be lower than estimated from the Tafel behavior. In other words, the currents seem to be reduced and limited by a slow diffusion of lithium across the surface layer and/or inside the electrode lattice. As may be seen from the figures, the Tafel curves move toward lower currents at low temperatures, indicating the sluggishness in the electrode kinetics. Also, the mass transfer interference appears to be less prominent at very low temperatures, possibly due to charge transfer kinetics also being considerably slower. It is interesting to note that the mass transfer interference seems to be more noticeable at moderately low temperatures, both for cathode as well as anode, which may be attributed to a relative hindrance in the charge transfer at low temperatures. A correction has therefore applied for these mass transfer effects by plotting logarithm of $I/(1 - I/I_{lim})$ against the electrode potential, instead of log (I),[20] where I_{lim} is the limiting current, obtained from an extrapolation to higher overpotentials, typically 500 mV. Figures 8a and 8b also contain the corrected Tafel plots for the anode and cathode, respectively, which are fairly linear over a sufficient range of currents. The kinetics parameters, i.e., exchange current density and the Tafel slopes, were calculated from the intercept and slope of the corrected Tafel plots for the processes of lithium deintercalation from the anode and

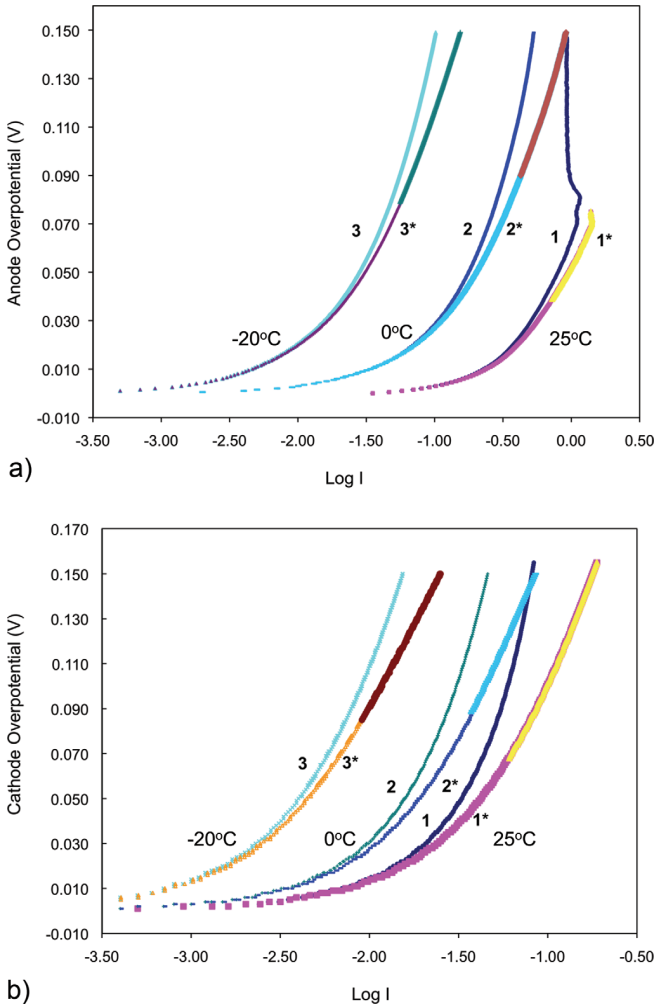

Figure 14. Tafel curves of (a) anode and (b) cathode in MCMB-NCO Li-ion test cells with electrolyte containing 1 M $LiPF_6$ in EC:DMC:DEC:EMC (1:1:1:4) without VC at (1) 25°C, (2) 0°C, and (3) –20°C. Also included here are the corresponding corrected (corrected for mass transfer effects) Tafel plots, designated as 1*, 2*, and 3*, respectively.

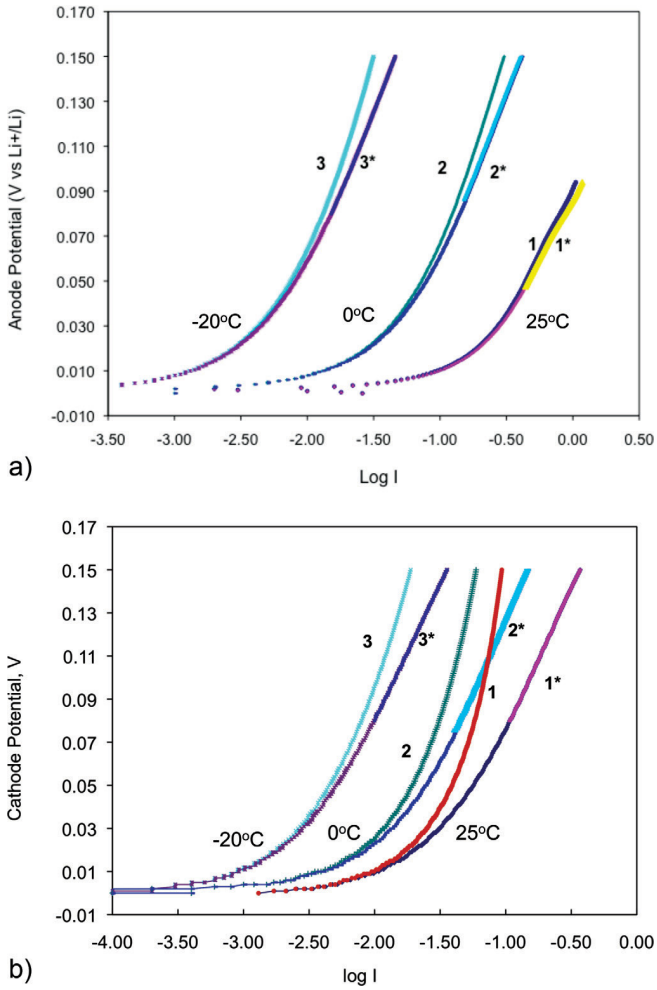

Figure 15. Tafel curves of (a) Anode and (b) Cathode in MCMB-NCO Li-ion test cells with electrolyte containing 1M $LiPF_6$ in EC:DMC:DEC:EMC (1:1:1:4) with VC additive at (1) 25°C, (2) 0°C, and (3) –20°C. Also included here are the corresponding corrected (corrected for mass transfer effects) Tafel plots, designated as 1*, 2*, 3* and 4* respectively.

intercalation into the cathode, respectively (Table I). The corresponding Tafel curves for the anode and cathode in the low-EC electrolyte solution are illustrated in Figs. 9a and 9b. The kinetic parameters calculated from these curves are also listed in Table I.

It is clear from Table I that the exchange currents decrease as the temperature is reduced, both for the anode and cathode reactions, in either high-EC or low-EC electrolytes. Further, the anode kinetics are less favorable in high-EC solution, while the cathode kinetics are favored in the high-EC formulation. A more quantitative analysis on these trends in electrode kinetics is provided in the latter sections.

Electrolyte formulations with "filming" additives.— In this example, an electrolyte additive, specifically vinylene carbonate (VC), which has been reported to assist in the formation of robust SEI on the anode[22] and thus contribute to an enhanced durability at warm temperatures,[23] has been studied in an electrolyte formulation containing a low proportion of ethylene carbonate. The electrolyte compositions examined include (i) 1.0 M $LiPF_6$ in EC+DEC+DMC+EMC (1:1:1:4 vol %) and (ii) 1.0 M $LiPF_6$ in EC+DEC+DMC+EMC (1:1:1:4 vol %) with ~1.5% of VC used as an electrolyte additive. The low-EC formulation, EC:DEC:DMC:EMC (1:1:1:4 vol %), has been demonstrated in our earlier studies to perform well at low temperatures.[24] A combination of this solvent mixture with small additions of VC is expected to provide the synergistic effect of good low temperature performance and enhanced high temperature resilience. Once again, three-electrode cells were fabricated with the above electrolyte solutions using MCMB anodes and lithiated nickel cobalt oxides cathodes, supplied by Yardney Technical products and Li reference electrodes, to derive basic electrochemical data on individual electrode kinetics at different temperatures.

Figure 10 shows the formation characteristics of these cells containing electrolytes based on the electrolyte without and with the VC additive, respectively. A comparison of their first lithiation process reveals that the anode SEI formation occurs more readily with the VC additive, as reported earlier.[5] Possibly due to such robust and thick SEI formed from the reduction of VC, the low temperature performance is slightly affected. Figure 11 illustrates the performance of cells in these two electrolytes at room temperature as well as at low temperature (–20°C), respectively. As may be expected, both the cells performed well at low temperatures, due to the use of low-EC solvent mixture.

There are more interesting differences between these two cells during charging, especially at low temperatures. Figure 12a shows the individual electrode potentials, cell voltage, and cell current during charging at 50 mA (C/10) at –20°C for the cells with and without the VC additive. The cathode exhibits a higher polarization in the electrolyte without the additive. In the electrolyte solution with the

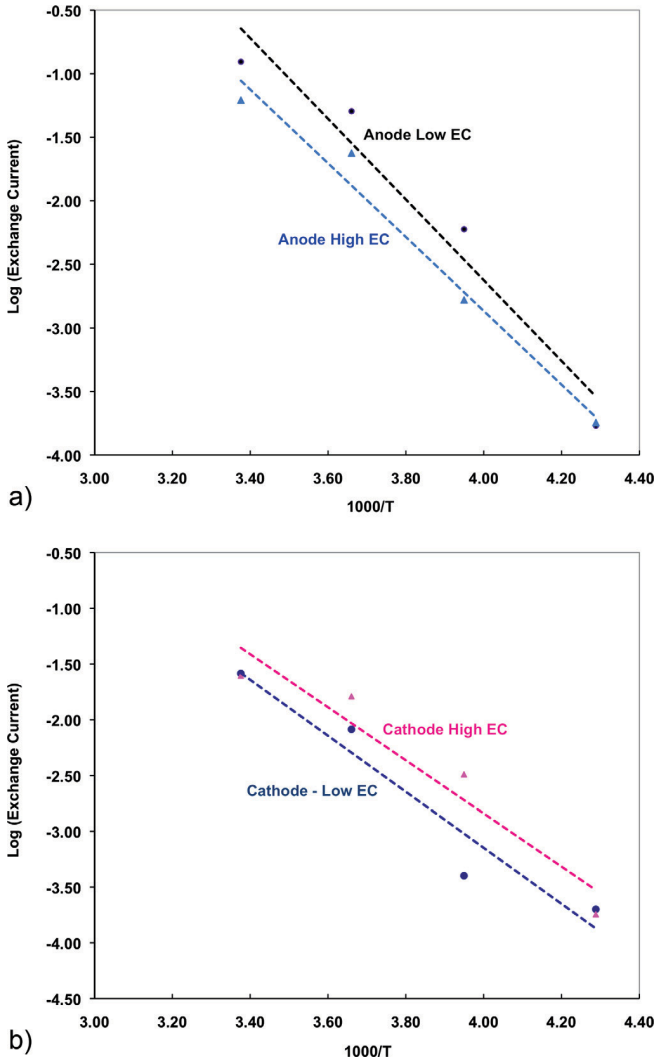

Figure 16. Activation energies for (a) Li intercalation in MCMB and (b) Li deintercalation in NCO in electrolytes containing 1M $LiPF_6$ in 1) High EC, i.e., 5:3:2 EC:DMC:EMC mixture and 2) Low EC, i.e., 1:1:1:4 EC:DMC:-DEC:EMC mixture.

VC additive, cathode potentials are lower by more than 50 mV, especially toward the end of constant-current charge and before the onset of taper. The anode potential, on other hand, exhibits the opposite trend. The anode potential remains anodic (positive) to Li^+/Li for the entire charge duration in the electrolyte without the VC additive. With the VC additive, however, the anode potential becomes negative for a considerable duration, even after the current is tapered. Based on these trends, we may expect to have lithium plating in the cell containing the VC additive, which is not readily apparent in the subsequent discharge (Fig. 12b). There is a high voltage plateau corresponding to lithium stripping in the cell containing the VC additive, but not evident in the cell without the additive. These disparities become more prominent at lower temperatures, as shown in Figs. 13a, –30 and –40°C (not shown here). At –30°C, the lowest anode potential during charge is about 50 mV negative to Li^+/Li in the electrolyte without the VC additive, compared to approximately –150 mV vs Li in the electrolyte containing the VC additive. Expectedly, the lithium plating is quite noticeable in the presence of the additive, evidenced by the high voltage plateau, whereas the cell without the additive shows no such voltage plateau. Similar trend is observed at –40°C also, with the cell without the VC additive showing no traces of Li plating, despite a little undershoot in the anode potential.

Electrode kinetics in solutions with and without VC additive.— Once again, for a quantitative understanding of the effects of the VC additive on the electrode kinetics, Tafel measurements were performed on the individual electrodes, in a similar fashion as described above. Figures 14a and 14b illustrate the Tafel polarizations of anode and cathode, respectively, in the formulation without any additive. Figures 15a and 15b illustrate the corresponding curves for the cell containing the VC additive. In all the Tafel plots, there is some inference from mass transfer processes on the charge transfer processes, which make them deviate from an ideal linear response between the overpotential and log (I). Once again, a correction was applied for these mass transfer effects by plotting logarithm of $I/(1 - I/I_{lim})$ against the electrode potential. The corrected Tafel plots are also displayed adjacent to the observed Tafel curves. The exchange current densities and the Tafel slopes calculated from the corrected Tafel plots are also listed in Table I. It is clear from Table I that the exchange currents decrease as the temperature is reduced in either case, both for the anode and cathode reaction. However, the anode kinetics are hindered by the addition of the VC additive, while the cathode kinetics appear to be improved. This finding is also consistent with our earlier study involving 1.0 M $LiPF_6$ EC+DEC+DMC+EMC (1:1:1:3) with and without the addition of 1.5% VC, in which the Li interaction kinetics were seen to improve at the cathode and degrade at the anode when in contact with the vinylene carbonate.[5] A more quantitative analysis on these exchange currents as a function of temperature is provided below.

Discussion

The performance of Li-ion cells is diminished at low temperatures due to (i) reduced ionic mobility of Li-ions (poor ionic conductivity and low diffusivity) in the electrolyte and in the SEI layer and ii) impaired kinetics for the charge transfer across the at the SEI covered electrodes. Our earlier studies reveal that a judicious optimization of the electrolyte, mainly its solvent composition, aids in the improvement of low temperature performance. Various successful electrolyte formulations were thus developed based on (i) reducing the EC content such that the viscosity is maintained low at low temperatures, while maintaining proper SEI characteristics and (ii) adding cosolvents that assist in further reducing the viscosity at low temperatures. Such successful candidate low-temperature electrolytes were found to improve not only the bulk properties but also create proper interfacial conditions that facilitate charge transfer processes. The two test cases being examined here include (i) electrolyte formulations with high-EC and low-EC proportions and (ii) (low-EC) electrolyte formulations with and without an SEI-stabilizing additive, VC. In addition to their ability to perform well at low temperatures, their tolerance against lithium plating during charging has been examined in terms of the electrode kinetics at these temperatures.

Between the electrolytes containing high-EC and low-EC proportions, we observed that the low temperature performance is superior in low-EC formulations. Also, there is less likelihood of lithium plating during low temperature charge in such electrolytes. An examination of their electrode kinetics (Fig. 16a) indicates that the anode kinetics are faster in the low-EC formulations, compared to the high-EC solutions. This improvement is more evident at lower temperature, similar to the discharge performance. Based on the Arrhenius plot, the activation energy for the anode charge transfer process is 14.3 kcal/mol in the low-EC formulation, compared to 13.2 kcal/mol in the high-EC solution (Table II). The cathode kinetics (Fig 16b), on the other hand, are superior in the high-EC electrolyte with nearly identical temperature dependence. The corresponding activation energies are 10.8 and 11.4 kcal/mol in the high-EC and low-EC solutions, respectively (Table II).

The effect of vinylene carbonate additions to the electrolyte has more interesting trends. This additive was originally proposed by Saft to have beneficial effect on the anode SEI. It is assumed to

Table II. Kinetic parameters for Li intercalation in graphite and deintercalation from NCO cathode in different electrolytes.

Electrolyte	Electrode	Arr. Slope	Activation energy, kcal/mol
1.0 M $LiPF_6$ in EC:DEC:DMC:EMC (1:1:1:3 vol %)	Anode	3.18	14.39
	Cathode	2.51	11.38
1.0 M $LIPF_6$ In EC+DMC+EMC (5:3:2 vol %)	Anode	2.90	13.16
	Cathode	2.38	10.79
1.0 M $LiPF_6$ in EC+DMC+DEC +EMC (1:1:1:4 vol%)	Anode	2.38	10.77
	Cathode	1.80	8.18
1.0 M $LIPF_6$ In EC+DEC+DMC +EMC (1:1:1:4 vol%)+VC	Anode	2.69	12.21
	Cathode	1.85	8.40

undergo "sacrificial reduction and polymerization" at the anode forming a robust SEI, which is expected to provide resilience to high temperature cycling and storage. Consistent with our earlier observations, the results here point to a more "inhibitive effect" on the anode kinetics. Figure 17a illustrates the difference in the anode kinetics with and without the VC additive in the low-EC formulations. The anode kinetics are vastly inhibited upon the addition the VC additive. This is probably the effect of the VC "decomposition product" over the SEI, which may provide the observed thermal protection, but contribute to some interfacial impedance or the kinetics.

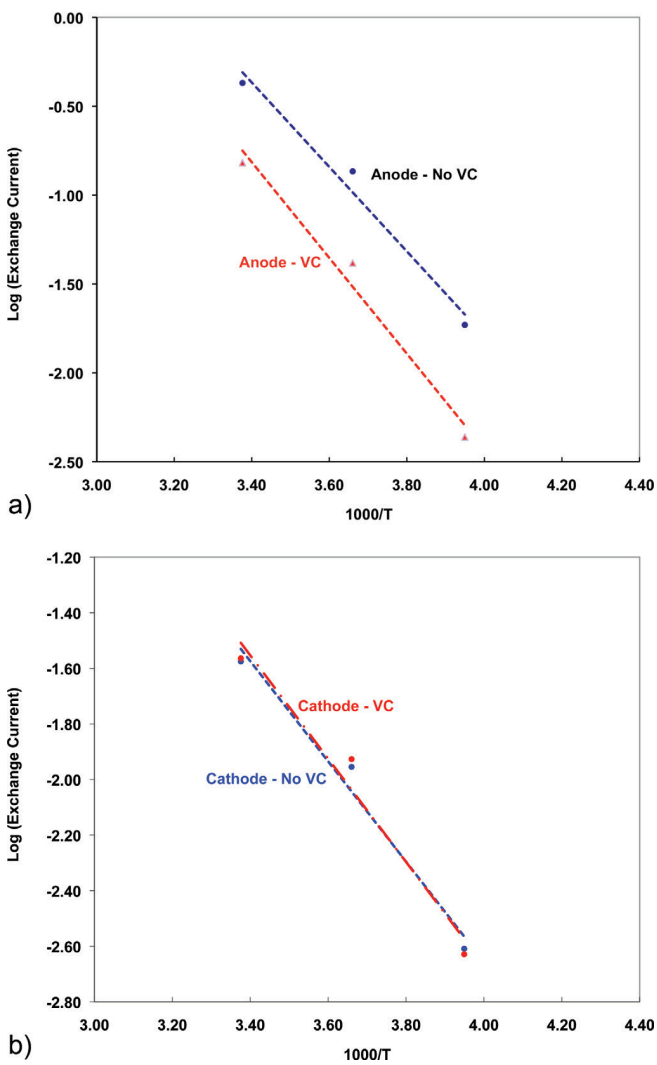

Figure 17. Activation energies for (a) Li intercalation in MCMB and (b) Li deintercalation in NCO in electrolytes containing 1M $LiPF_6$ in EC:DMC:DEC:EMC (1:1:1:4) and 1) with and 2) without the VC additive.

The corresponding activation energies are 10.8 and 12.2 kcal/mol for the cells without and with the VC additive. The cathode kinetics are quite similar in solutions with and without the additive, with the activation energies of 8.2 and 8.4 kcal/mol (Fig. 17b).

Based on the above discussions of the electrode kinetics in these solutions and their susceptibility toward lithium plating, it is clear that in all cases, where there is an inhibition of the lithium intercalation kinetics in the anode, either from the presence of high proportion of EC in the electrolyte or with the "SEI-stabilizing" additives, there is a greater likelihood for lithium plating.

Conclusions

Lithium plating on the graphite anode is a parasitic process that accompanies lithium intercalation, during strenuous charge conditions, i.e., high charge rates and low charge temperatures. Such plated lithium is deleterious to the performance, reliability, and even safety of Li-ion cells. Lithium plating may be a result of faulty design of cell relative to anode and cathode dimensions and capacities, as well as improper use of the batteries. Several design parameters such as the nature of electrode and electrolyte materials and the amount of anode reserve dictate the susceptibility to lithium plating. There is a strong correlation between the intercalation kinetics and the plating behavior, as demonstrated here in two different examples, i.e., solutions with high- and low-EC formulations and electrolytes with and with anode-filming additives. Specifically, the electrolytes containing high-EC formulations and those with SEI-stabilizers such as VC enable the formation of form a tenacious SEI, which may impede lithium intercalation into graphite at low temperature and thus pave the way for lithium plating. A judicious selection of electrolyte is thus one of the options to mitigate the plating and the associated failures.

Acknowledgments

The work described here was carried out at the Jet Propulsion Laboratory, California Institute of Technology, for the Advanced Battery program sponsored by the NASA's Chief Engineer's Office, under contract with the National Aeronautics and Space Administration (NASA).

Jet Propulsion Laboratory assisted in meeting the publication costs of this article.

References

1. T. Nagura and K. Kozawa, *Prog. Batteries Sol. Cells*, **9**, 209 (1990).
2. D. W. Murphy and P. A. Christian, *Science*, **205**, 651 (1979).
3. M. C. Smart, B. V. Ratnakumar, S. Surampudi, Y. Wang, X. Zhang, and S. G. Greenbaum, *J. Electrochem. Soc.*, **146**, 3963 (1999).
4. A. Hightower, C. C. Ahn, and B. Fultz, *Appl. Phys. Lett.*, **77**, 238 (2000).
5. M. C. Smart, B. V. Ratnakumar, L. Whitcanack, K. B. Chin, M. Rodrigues, S. Surampudi, H. Croft, D. Tice, and R. Staniewicz, *IEEE Aerospace and Electronic System Magazine*, **119–121**, 349 (2003).
6. P. Aurora, M. Doyle, and R. E. White, *J. Electrochem. Soc.*, **146**, 3543 (1999).
7. E. Scott, G. Tam, B. Anderson, and C. Schmidt, Paper 1282, presented at The Electrochemical Society Meeting, Orlando, FL, Oct 13, 2003.
8. M. Tang, P. Albertus, and J. Newman, *J. Electrochem. Soc.*, **156**, A 390 (2009).
9. A. H. Whitehead, M. Perkins, and J. R. Owen, *J. Electrochem., Soc.*, **144**, L92 (1997).
10. J. Fan and S. Tan, *J. Electrochem. Soc.*, **153**, A1081 (2006).
11. M. C. Smart, B. V. Ratnakumar, and S. Surampudi, *J. Electrochem. Soc.*, **146**, 486 (1999).

12. S. S. Zhang, K. Xu, and T. R. Jow, *J. Power Sources*, **160**, 1349 (2006).
13. S. J. Harris, A. Timmons, D. R. Baker, and C. Monroe, *Chem. Phys. Lett.*, **485**, 265 (2010).
14. B. V. Ratnakumar and M. C. Smart, *ECS Trans.*, **25**(36), 241(2010).
15. M. Broussely, Ph. Biensan, F. Bonhomme, Ph. Blanchard, S. Herreyre, K. Nechev, and, R. J. Staniewicz, *J. Power Sources*, **146**, 90 (2005).
16. C. J. Mikolajczak, J. Harmon, P. Golpalakrishnan, R. Gogithi, and M. Wu, in *NASA Battery Workshop*, Huntsville, AL, Nov 19, 2009.
17. B. V. Ratnakumar, M. C. Smart, and S. Surampudi, *J. Power Sources*, **97–98**, 137 (2001).
18. J. R. Dahn, A. K. Sleigh, H. Shi, J. N. Reimers, Q. Zhong, and B. M. Way, *Electrochim. Acta*, **38**, 1179 (1993).
19. T. Zheng, J. N. Reimers, and J. R. Dahn, *Phys. Rev. B*, **51**, 734 (1995).
20. M. C. Smart, B. V. Ratnakumar, and S. Surampudi, *J. Electrochem. Soc.*, **149**, A361 (2002).
21. A. J. Bard and L. R. Faulkner, *Electrochemical Methods, Fundamentals and Applications*, John Wiley & Sons, New York (1980).
22. B. Simon and J. P. Boeuve, U.S. Pat. 5,626,981 (1997).
23. D. Aurbach, K. Gamolsky, B. Markovsky, Y. Gofer, M. Schmidt, and U. Heider, *Electrochim. Acta*, **47**, 1423 (2002).
24. M. C. Smart, B. V. Ratnakumar, L. Whitcanack, K. Chin, and S. Surampudi, H. Croft, D. Tice and R. Staniewicz, *J. Power Sources*, **119–121**, 349 (2003).